Original Article

Integrative analysis of the role of the *DPH* gene family in hepatocellular carcinoma and expression validation

Xiaojin Gao[1,2#], Kun He[1,2,3#], Zhongxiang Zeng[1,2], Yaolin Yin[1], Jie Huang[1,2], Xingliang Liu[1,2], Xiaocong Xiang[1,2], Jingdong Li[1,2]

[1]Institute of Hepato-Biliary-Pancreatic-Intestinal Disease, Affiliated Hospital of North Sichuan Medical College, Nanchong, China; [2]Department of Hepatobiliary Surgery, Academician (Expert) Workstation, Affiliated Hospital of North Sichuan Medical College, Nanchong, China; [3]Department of Hepatobiliary Surgery, Jintang Second People's Hospital, Chengdu, China

Contributions: (I) Conception and design: X Gao, K He, X Xiang; (II) Administrative support: Y Yin, J Li; (III) Provision of study materials or patients: X Xiang, J Li; (IV) Collection and assembly of data: Z Zeng, J Huang; (V) Data analysis and interpretation: X Gao, X Liu, K He; (VI) Manuscript writing: All authors; (VII) Final approval of manuscript: All authors.

[#]These authors contributed equally to this work.

Correspondence to: Xiaocong Xiang, PhD; Jingdong Li, MD. Institute of Hepato-Biliary-Pancreatic-Intestinal Disease, Affiliated Hospital of North Sichuan Medical College, No. 234 Fuljiang Road, Shunqing District, Nanchong 637000, China; Department of Hepatobiliary Surgery, Academician (Expert) Workstation, Affiliated Hospital of North Sichuan Medical College, Nanchong, China. Email: xiaocongx@nsmc.edu.cn; lijingdong358@nsmc.edu.cn.

Background: The diphthamide (*DPH*) gene family is a group of genes that encode a set of enzymes that specifically modify eukaryotic elongation factor 2 (eEF2). Although previous studies have shown a link between the *DPH* genes (*DPHs*) and carcinogenesis, it is still unknown how the *DPHs* affect hepatocellular carcinoma (HCC). This study aimed to describe the expression, clinical significance, and potential mechanisms of *DPHs* in HCC.

Methods: Real-time quantitative polymerase chain reaction (RT-qPCR), Genotype-Tissue Expression (GTEx), and The Cancer Genome Atlas (TCGA) databases were utilized to research the expression of DPHs in HCC. The relationship between the expression of *DPHs* and the clinicopathological characteristics of HCC patients was investigated using TCGA data, and their diagnostic value was evaluated using receiver operating characteristic (ROC) curves and their prognostic value was analyzed using Kaplan-Meier curves and univariate and multivariate Cox regression analyses. Potential reasons for the upregulation of *DPH2* and *DPH3* (*DPH2,3*) expression in HCC were analyzed using multiple databases. Additionally, this study also explored the potential biological functions of *DPH2,3* in HCC via gene sets enrichment analysis (GSEA). Correlation analysis of *DPH2,3* expression with immune-related genes and immune checkpoints was performed using Spearman's correlation analysis, and single-sample GSEA was used to assess the distribution of tumor-infiltrating immune cell types.

Results: *DPH1,7* expression was downregulated in tumor tissues while *DPH2,3,5,6* expression was upregulated and showed a similar expression pattern in HCC. The results of the ROC analysis suggested that *DPHs* had valuable diagnostic properties in HCC. Kaplan-Meier analysis demonstrated that *DPH2,3,7* had prognostic predictive value in HCC. Furthermore, univariate and multivariate Cox regression suggested that *DPH2,3* was an independent predictive factor for HCC. GSEA analysis revealed that *DPH2,3* might be tightly associated with Pathways in cancer, cell cycles, Fc gamma R mediated phagocytosis, etc. Additionally, *DPH2,3* expression and numerous immune-related genes showed a positive connection, including chemokines receptor genes, immunosuppressive genes, chemokines genes, human leukocyte antigen (HLA) genes, and immunostimulatory genes. Further analysis of the association between 24 immune infiltrating cells and *DPH2,3* revealed the greatest negative correlation between natural killer (NK) cells and Th17 cells, but the greatest positive correlation with Th2 cells.

Conclusions: *DPHs* significantly influence the development and progression of HCC. *DPH2,3* has significant diagnostic and prognostic potential and may be a promising target for immunotherapy.

Keywords: Diphthamide gene family (*DPH* gene family); hepatocellular carcinoma (HCC); tumor microenvironment (TME); immune checkpoints; immune cells

Submitted Jan 22, 2024. Accepted for publication Jul 09, 2024. Published online Aug 26, 2024.
doi: 10.21037/tcr-24-147
View this article at: https://dx.doi.org/10.21037/tcr-24-147

Introduction

Hepatocellular carcinoma (HCC) accounts for a large majority of liver cancer cases, and it is one of the leading causes of cancer-related deaths worldwide (1,2). Sadly, only 18% of HCC patients survive for at least 5 years, which indicates a poor prognosis (3). There are several treatment options available for individuals with HCC, such as surgical resection and liver transplantation, as well as transarterial, radiotherapy, and percutaneous ablation. However, systemic therapy has become the preferred treatment for those with intermediate to advanced disease or individuals who are not eligible for local treatment (4). Long-term survival of more than a year is still unusual, although systemic medication therapy has lately given hope for the treatment of HCC patients a new lease of life (5). Immunotherapy is crucial in treating HCC and can synergize with other treatments (6-8). Biomarkers play a vital role in precision medicine by helping to identify the most effective treatment options (4,9). Therefore, novel biomarker studies are essential for early detection, treatment, and prognosis follow-up of HCC.

The diphthamide (*DPH*) gene family members, including *DPH1*, *DPH2*, *DPH3*, *DPH5*, *DPH6*, and *DPH7*, produce enzymes that play a crucial role in creating diphthamide. Diphthamide is a modified form of histidine that is only found in eukaryotic elongation factor 2 (eEF2). These post-translational modifications are critical in ensuring the accuracy and efficiency of the translation process (10). However, diphthamide is the target of pseudomonas exotoxin and diphtheria toxin ADP-ribosylation, halting protein synthesis and causing cell death (11-13). The "active state" of diphthamide directly affects the immunotoxicity of tumor cells, in which the *DPH* genes (*DPHs*) play an indispensable role (14). Studies have shown that *eEF2* overexpression promotes the proliferation, migration, and invasion of a wide range of tumors (15) and may be a potential target for drug therapy (16). Recent studies have shown that *DPH1* deletion or deletion of diphthamide inhibits the development of N-diethylnitrosamine (DEN)-induced periportal HCC, but leads to an increase in K19-positive periportal stem, progenitor cells, which nevertheless promotes Pten, Trp53-deficient HCC development (17). In addition, colorectal cancer cells affect their proliferation and invasion through the MiR218-5p, *DPH1* axis (18). Mutations in the *DPH3* gene have been associated with basal cell carcinoma (19,20). And fusions of the *DPH7* and *PTP4A3* genes may be associated with tumor grading and recurrence in endometrial cancer (21). However, the specific role of *DPHs* in HCC is unclear.

Our primary objective was to analyze the expression patterns of *DPHs* in HCC. Moreover, we investigated their diagnostic and prognostic value in HCC patients and their associated clinical features. Our research revealed that *DPH2* and *DPH3* (*DPH2,3*) are independent prognostic

Highlight box

Key findings

- Diphthamide genes (*DPHs*) are significantly differentially expressed in cancer, particularly in hepatocellular carcinoma (HCC).
- *DPH2,3* demonstrated significant diagnostic and prognostic potential in HCC, with strong correlations to various immune-related genes and tumor-infiltrating immune cells, suggesting a role in immune modulation.

What is known and what is new?

- It is known that the diphthamide (*DPH*) gene family modifies eukaryotic elongation factor 2 (*eEF2*) and is linked to carcinogenesis.
- This study provides new insights into the roles of *DPH2,3* in HCC, highlighting their expression patterns and diagnostic and prognostic relevance, as well as their potential mechanisms related to immune-related genes and pathways.

What is the implication, and what should change now?

- The findings suggest that *DPH2,3* could serve as valuable biomarkers for the diagnosis and prognosis of HCC.
- The expression of *DPH2,3* should be further explored as potential therapeutic targets, particularly in the context of immunotherapy. Given their association with immune-related genes and pathways, *DPH2,3* hold promise for enhancing the efficacy of immunotherapies in HCC, potentially leading to more effective treatment strategies.

factors for HCC patients. We also delved into the methylation and mutation of *DPH2,3* in HCC to determine the reasons for its increased expression. After analyzing the reasons for the increased expression of *DPH2,3*, we conducted a gene sets enrichment analysis (GSEA) and discovered a potential connection between *DPH2,3* and the tumor microenvironment (TME). We further examined the role of *DPH2,3* in TEM by studying its relationship with immune-related genes and immune-infiltrating cells. The research suggests a strong link between HCC and *DPHs*, with *DPH2,3* being a possible target for treating HCC. The theoretical basis of our current work contributes to the development of a new effective molecular pathway for the treatment of HCC. We present this article in accordance with the MDAR reporting checklist (available at https://tcr.amegroups.com/article/view/10.21037/tcr-24-147/rc).

Methods

Ethical statement

The research conducted has adhered to the moral guidelines set in the Declaration of Helsinki (as revised in 2013) by the World Medical Association while acquiring and classifying all human tissue samples. The study was approved by The Medical Ethics Committee of the Affiliated Hospital of North Sichuan Medical College (protocol No. 2023ER153-1). All patients who participated in the study provided written informed consent before the collection of tissue samples.

Clinical samples

All tissue samples were collected in November 2019 and June 2020. Patients over 18 who had undergone surgical resection of the primary tumor and were confirmed to have HCC through pathology assessment were included. All tissue samples were obtained from the Affiliated Hospital of North Sichuan Medical College's Department of Hepatobiliary Surgery. None of the study participants had received any radiation, chemotherapy, or immunotherapy therapies before surgery. Two independent pathologists independently verified the identification of each material to guarantee correct post-surgical diagnosis. The tissue samples were immediately submerged in liquid nitrogen following collection and were stored at −80 ℃. All tissue samples are stored at the Hepato-Biliary-Pancreatic-Intestinal Disease Department of the North Sichuan Medical College.

Cell culture

HCC cell lines, including Huh7, Hep3B, HepG2, SMMC7721, HCCLM3, MHCC97L, and MHCC97H, were obtained from the Cell Bank of the Chinese Academy of Sciences (Shanghai, China). The Huh7, Hep3B, HepG2, HCCLM3, MHCC97L, and MHCC97H cell lines were cultured in DMEM (VivaCell, Shanghai, China) supplemented with 10% fetal bovine serum (VivaCell). While the SMMC7721 cell line was cultured in RPMI-1640 medium (VivaCell) supplemented with 10% fetal bovine serum. They were cultured at 37 ℃ and 5% CO_2 under recommended conditions. Only the cells in the logarithmic growth phase were collected for subsequent experiments.

Real-time quantitative polymerase chain reaction (RT-qPCR)

Total RNAs were isolated from the samples using Trizol reagent (Invitrogen, Waltham, MA, USA). The RNA was then extracted with chloroform, isopropanol, and alcohol. The extracted RNA was reverse transcribed to complementary DNA (cDNA) using a HiScript III RT SupperMix for Qpcr (+gDNA wiper) kit (Vazyme Biotech, Nanjing, China). RT-qPCR was performed using Taq Pro Universal SYBR qPCR Master Mix kit (Vazyme Biotech). The relative expression of DPHs mRNA was calculated using the delta-delta Cq ($2^{-\Delta\Delta Ct}$) method with GAPDH as the internal control. The specific primers (Sangon Biotech, Chengdu, China) used for amplifying each gene are listed in *Table 1*.

Data sources and processing

We obtained RNA-seq data in transcripts per-million (TPM) format for The Cancer Genome Atlas (TCGA) and Genotype-Tissue Txpression (GTEx) from the UCSC XENA (https://xenabrowser.net/) using the Toil process (22). We extracted (pan-cancer) data corresponding to TCGA and the corresponding normal tissue data in GTEx. The full names and abbreviations of the pan-cancers are shown in *Table 2*. We downloaded RNA-seq data from the TCGA database (https://www.cancer.gov/ccg/research/genome-sequencing/tcga) for the STAR process of the TCGA-LIHC project and extracted data in TPM format and clinical data. Depending on the characteristics of the data format, we selected appropriate statistical methods for analysis using R packages "stats" (version 4.2.1) and "car" (version 3.1.0), and visualized the data using the

Table 1 The sequences of RT-qPCR primers

Primer name	Sequence
DPH1	
Forward	CTGAAAGCCGAGTATCGTGTG
Reverse	TGTTCTCTGGATAGGACTTTGCT
DPH2	
Forward	CCTGGACGGAGTGTACGAG
Reverse	AGCATCTCCCAATAGCTGGTC
DPH3	
Forward	GCAGTGTTTCATGACGAGGTG
Reverse	TTGCCACGTCTTCCCCATTC
DPH5	
Forward	ATGCTTTATCTCATCGGGTTGG
Reverse	GCAGCGTCTAACAACTTCCAG
DPH6	
Forward	TGCTGGGCATCAGATCGTTG
Reverse	GAGGGGAAGAGCCATTGCTT
DPH7	
Forward	AGCCTCAGGTCCGTTTAGG
Reverse	CCTCGACCAGAGGGTGAATAG
GAPDH	
Forward	GGAGCGAGATCCCTCCAAAAT
Reverse	GGCTGTTGTCATACTTCTCATGG

RT-qPCR, real-time quantitative polymerase chain reaction; *DPH*, diphthamide.

ggplot2 (version 3.3.6) package. To ensure accuracy and consistency, we transformed these values by $\log_2$(TPM + 1) (22). We retrieved immunohistochemistry (IHC) and immunofluorescence images from the Human Protein Atlas (HPA) database (https://www.proteinatlas.org/) to assess expression levels and subcellular localization of DPHs proteins in HCC (23). Additionally, Information about DPHs protein expression was obtained from the University of Alabama Cancer database (UALCAN) (https://ualcan.path.uab.edu/index.html) (24).

The relationship between clinicopathological characteristics and DPHs mRNA

We analyzed the clinical data from 374 HCC patients in

Table 2 Full names and abbreviations of the 33 cancers in the TCGA database

Abbreviations	Full names
ACC	Adrenocortical carcinoma
BLCA	Bladder urothelial carcinoma
BRCA	Breast invasive carcinoma
CESC	Cervical squamous cell carcinoma and endocervical adenocarcinoma
CHOL	Cholangiocarcinoma
COAD	Colon adenocarcinoma
DLBC	Lymphoid neoplasm diffuse large B-cell lymphoma
ESCA	Esophageal carcinoma
GBM	Glioblastoma multiforme
HNSC	Head and neck squamous cell carcinoma
KICH	Kidney chromophobe
KIRC	Kidney renal clear cell carcinoma
KIRP	Kidney renal papillary cell carcinoma
LAML	Acute myeloid leukemia
LGG	Lower grade glioma
LIHC	Liver hepatocellular carcinoma
LUAD	Lung adenocarcinoma
LUSC	Lung squamous cell carcinoma
MESO	Mesothelioma
OV	Ovarian serous cystadenocarcinoma
PAAD	Pancreatic adenocarcinoma
PCPG	Pheochromocytoma and paraganglioma
PRAD	Prostate adenocarcinoma
READ	Rectum adenocarcinoma
SARC	Sarcoma
SKCM	Skin cutaneous melanoma
STAD	Stomach adenocarcinoma
TGCT	Testicular germ cell tumor
THCA	Thyroid carcinoma
THYM	Thymoma
UCEC	Uterine corpus endometrial carcinoma
UCS	Uterine carcinosarcoma
UVM	Uveal melanoma

TCGA, The Cancer Genome Atlas.

the TCGA database, to investigate the correlation between *DPHs* mRNA expression levels and clinicopathological characteristics, such as T, N, M stage, pathologic stage, gender, age, height, body mass index (BMI), prothrombin time, and vascular invasion. We used R and appropriate statistical methods to analyze the relationship between the expression of *DPH* genes and relevant clinical data.

The diagnostic and prognostic value of DPHs in HCC

We carried out an in-depth study to assess the diagnostic and prognostic significance of *DPHs* in HCC using data obtained from the TCGA. We used receiver operating characteristic (ROC) analysis with the R package "pROC" (version 1.18.0) and calculated the area under the curve (AUC). Next, we divided the cases into two groups (high-expression and low-expression groups) based on the median expression values of *DPHs* mRNA. We used the "survival" (version 3.3.1) R package to perform proportional risk hypothesis testing and fit survival regressions. This allowed us to make a comparison between the overall survival (OS) of the two groups. We then executed proportional risk hypothesis testing using the R package "survival" (version 3.3.1) and "rms" (version 6.3.0). We used TNM stage, pathologic stage, gender, age, and *DPHs* as statistical variables for Cox regression analysis (when the univariate analysis met P<0.1, it was entered into a multivariate COX to construct the model) (25).

Mutation and DNA methylation analysis of DPH2,3 in HCC

The analysis of mutations and gene amplifications in 1348 HCC samples was conducted using the cBioPortal database (https://www.cbioportal.org/). The samples were sourced from reputable institutions such as "Peking University, Cancer Cell 2019", "INSERM, Nat Genet 2015", "AMC, Hepatology 2014", "RIKEN, Nat Genet 2012", "MERiC, Basel, Nat Commun, 2022", "MSK, Clin Cancer Res 2018", and "TCGA Firehose Legacy", were utilized for the analysis of mutations and gene amplifications (26). We retrieved mutations and copy number alterations in the *DPH2,3* genes in HCC from the cBioPortal database. Furthermore, we used the UALCAN database to examine the promoter methylation status of *DPH2,3* in HCC (24). Additionally, MethSurv (https://biit.cs.ut.ee/methsurv/) was utilized for prognostic analysis related to the methylation probes of *DPH2,3* (27).

GSEA of DPH2,3 in HCC

We used GSEA (28) to explore the mechanism behind the high expression of DPH2,3 in HCC (29). First, line ID conversion was performed using the R package "rg.Hs.eg.db", followed by GSEA analysis using the "clusterProfiler" package (version 4.4.4) (30). The significance thresholds were set at P<0.05 and q<0.25. From the MSigDB collection (https://www.gsea-msigdb.org/gsea/msigdb), we selected "c2.cp.all.v2022.1.Hs.symbols.gmt" as the reference gene set for pathway analysis. Finally, we chose the Kyoto Encyclopedia of Genes and Genomes (KEGG) pathway from the MSigDB collection for presentation.

Relationship analysis between immune-related genes and immune cell infiltration in DPH2,3

We performed correlation analyses of the variables in the data and the results were visualised in heatmaps and scatterplot to investigate the correlation between *DPH2,3* and immune-related genes. We analyzed the immune infiltration of *DPH2,3* based on the "ssGSEA" algorithm provided in the R package "GSVA" (version 1.46.0) in combination with 24 markers of immune cells provided in the immunity article (31,32).

Statistical analysis

The data was analyzed and visualized using R (version 4.2.1) and GraphPad (version 8.0.1). We conducted an analysis of the expression of *DPHs* in various types of cancer, including HCC. To do this, we used the Wilcoxon rank sum test to compare gene expression levels. For two-sample data, we utilized paired *t*-tests, and for multiple-sample data, we used one-way ANOVA. In order to assess the correlation between the gene expression levels of *DPHs* and clinical characteristics, we chose the appropriate statistical methods based on the characteristics of the data. To predict the prospects of *DPHs* as diagnostic biomarkers, we performed ROC curve analysis with the pROC R package. We also analyzed the OS of *DPHs* in HCC using the Log-rank test. To study the correlation of *DPH2,3* with immune-related genes and immune cells, we used Spearman. Additionally, we compared the difference in immune infiltrating cells between high and low *DPH2,3* expression groups using the Wilcoxon rank sum test. We defined P<0.05 as statistically significant.

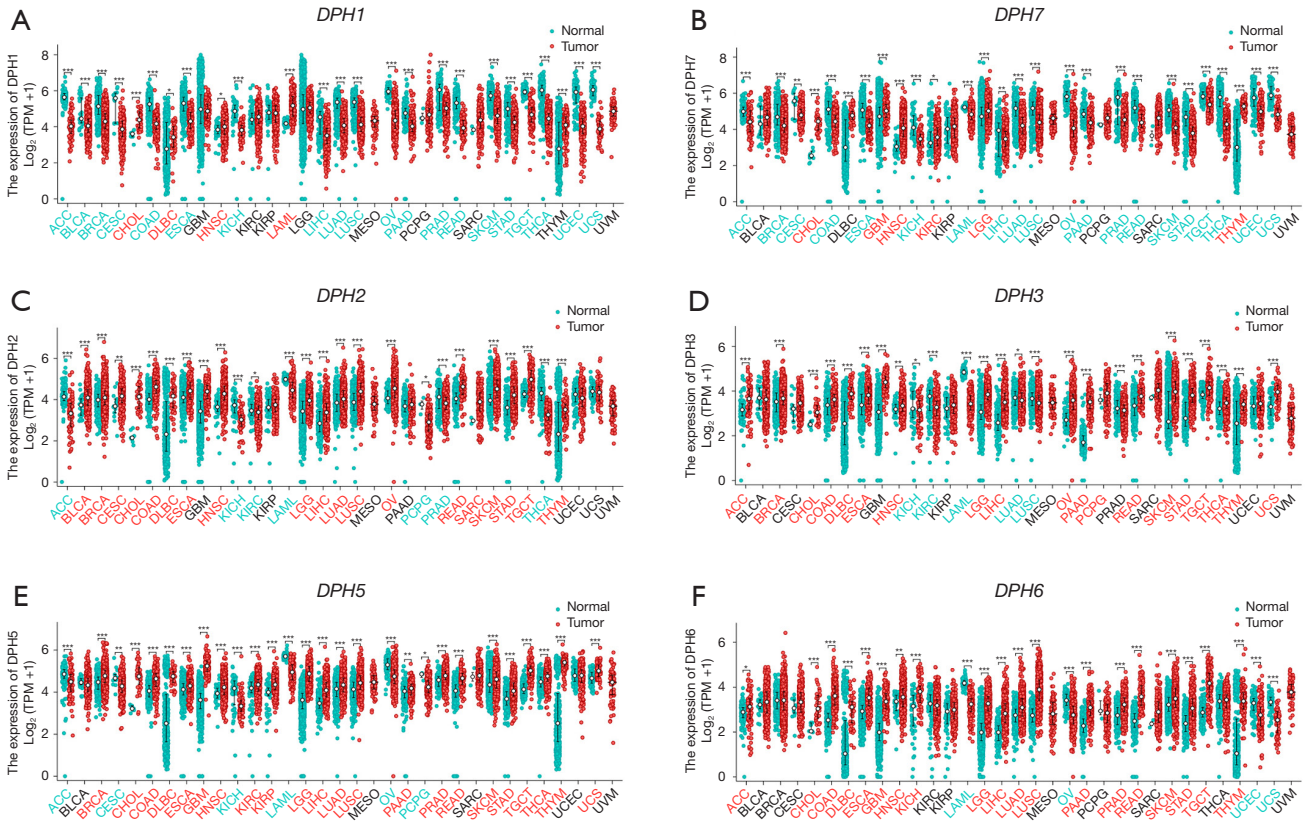

Figure 1 The expression of *DPHs* in pan-cancer. (A) *DPH1*; (B) *DPH7*; (C) *DPH2*; (D) *DPH3*; (E) *DPH5*; (F) *DPH6*. *, P<0.05; **, P<0.01; ***, P<0.001. Blue indicates that normal tissue exhibits higher levels of expression than cancerous tissue, whereas red indicates that cancerous tissue exhibits higher levels of expression than normal tissue in the X-axis typeface. *DPHs*, *DPH* genes; TPM, transcripts per-million; *DPH*, diphthamide.

Results

Patterns of DPHs expression in pan-cancer and HCC

We conducted a thorough pan-cancer analysis of the *DPHs* using the TCGA-GTEx pan-cancer dataset, looking at the mRNA expression levels in 33 distinct cancer types. Our findings demonstrated that *DPH1*,7 was considerably downregulated in 20 tumors, including adrenocortical carcinoma (ACC), breast invasive carcinoma (BRCA), and liver hepatocellular carcinoma (LIHC). However, *DPH1*,7 was overexpressed in head and neck squamous cell carcinoma (HNSC), lymphoid neoplasm diffuse large B-cell lymphoma (DLBC), and cholangiocarcinoma (CHOL) (*Figure 1A*,*1B*). *DPH2*,*3*,*5*,*6* showed significant overexpression in a broad variety of cancer types, including 17 malignancies such as BRCA, CHOL, and LIHC, except acute myeloid leukemia (LAML) and kidney chromophobe (KICH) (*Figure 1C-1F*). These data implied that *DPH2*,*3*,*5*,*6*, which consistently overexpressed across a broad range of malignancies, may be crucial in the formation of carcinogenesis and tumors. On the other hand, *DPH1*,7 was downregulated in a variety of cancers.

TCGA database RNA-seq data paired analysis revealed that *DPHs* were considerably increased in HCC (*Figure 2A*). *DPH2*,*3*,*5*,*6* were significantly overexpressed in HCC, according to an unpaired analysis, while *DPH1*,7 showed significantly downregulated expression (*Figure 2B*). *DPH2*,*3*,*5*,*6* protein were significantly increased in HCC, while *DPH1*,7 protein were expressed at lower levels, according to IHC data from the HPA database. The UALCAN database displays the total protein expression of the *DPHs*, with *DPH1*,*2*,*3*,*5* expression being up-regulated in HCC and *DPH7* expression being down-regulated (*Figure 2C*). Overall, between normal and HCC tissues, there were considerable differences in the mRNA and protein expression of *DPHs*.

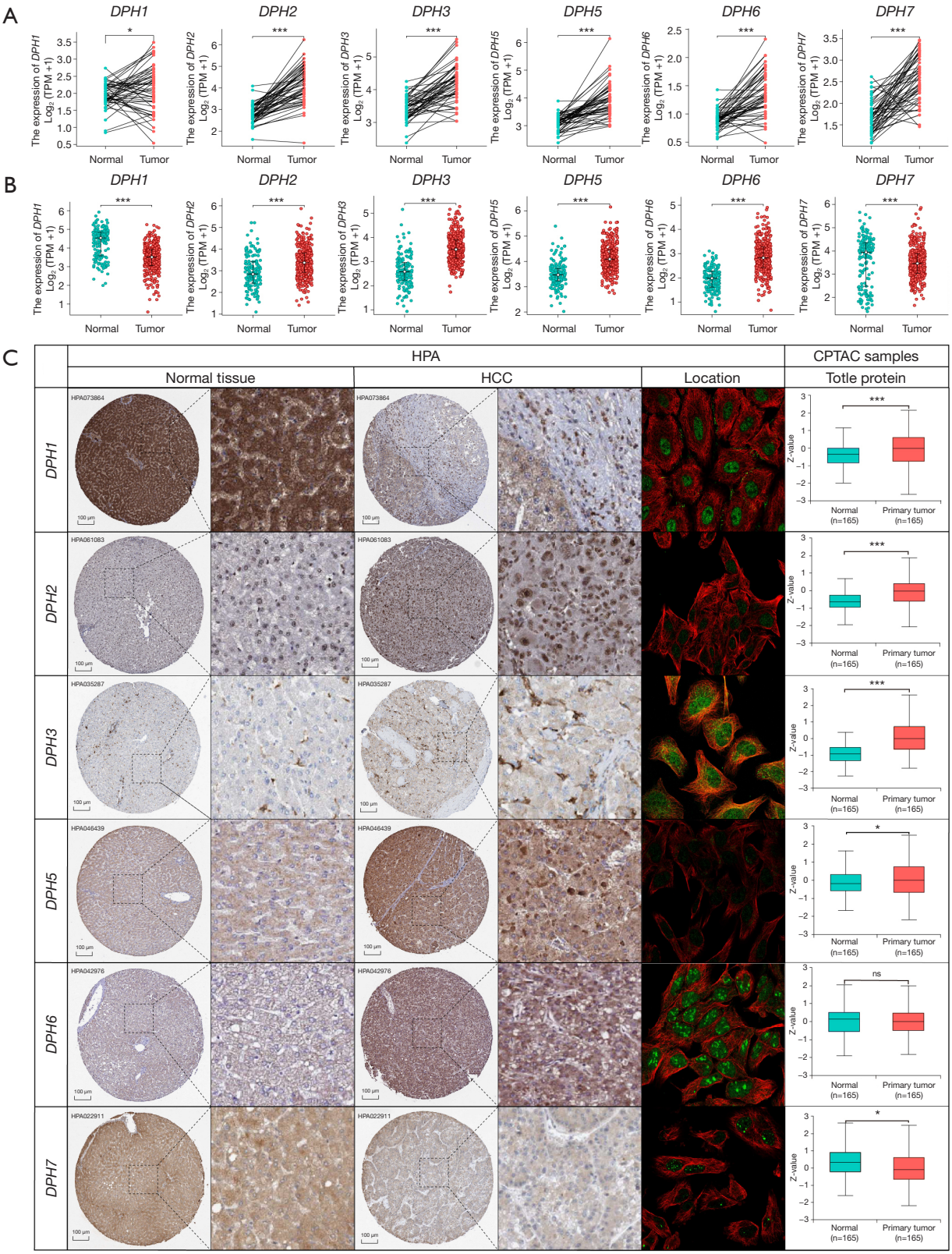

Figure 2 *DPHs* mRNA and protein expression in HCC. (A,B) Expression of *DPHs* mRNA in HCC and normal tissues (paired and unpaired); (C) protein expression and immunofluorescence localization data of *DPHs* in HPA and UALCAN, CPTAC databases (HPA:

immunohistochemistry ×40 images are presented). *DPH1* (normal tissue: https://www.proteinatlas.org/ENSG00000108963-DPH1/tissue/liver; HCC: https://www.proteinatlas.org/ENSG00000108963-DPH1/pathology/liver+cancer); *DPH2* (normal tissue: https://www.proteinatlas.org/ENSG00000132768-DPH2/tissue/liver; HCC: https://www.proteinatlas.org/ENSG00000132768-DPH2/pathology/liver+cancer); *DPH3* (normal tissue: https://www.proteinatlas.org/ENSG00000154813-DPH3/tissue/liver; HCC: https://www.proteinatlas.org/ENSG00000154813-DPH3/pathology/liver+cancer); *DPH5* (normal tissue: https://www.proteinatlas.org/ENSG00000117543-DPH5/tissue/liver; HCC: https://www.proteinatlas.org/ENSG00000117543-DPH5/pathology/liver+cancer); *DPH6* (normal tissue: https://www.proteinatlas.org/ENSG00000134146-DPH6/tissue/liver; HCC: https://www.proteinatlas.org/ENSG00000134146-DPH6/pathology/liver+cancer); *DPH7* (normal tissue: https://www.proteinatlas.org/ENSG00000148399-DPH7/tissue/liver; HCC: https://www.proteinatlas.org/ENSG00000148399-DPH7/pathology/liver+cancer). Subcellular location images are presented. *DPH1*: https://www.proteinatlas.org/ENSG00000108963-DPH1/subcellular; *DPH2*: https://www.proteinatlas.org/ENSG00000132768-DPH2/subcellular; *DPH3*: https://www.proteinatlas.org/ENSG00000154813-DPH3/subcellular; *DPH5*: https://www.proteinatlas.org/ENSG00000117543-DPH5/subcellular; *DPH6*: https://www.proteinatlas.org/ENSG00000134146-DPH6/subcellular; *DPH7*: https://www.proteinatlas.org/ENSG00000148399-DPH7/subcellular. ns, P≥0.05; *, P<0.05; ***, P<0.001. *DPHs*, *DPH* genes; HCC, hepatocellular carcinoma; HPA, Human Protein Atlas; UALCAN, The University of Alabama Cancer database; CPTAC, Clinical Proteomic Tumor Analysis Consortium; TPM, transcripts per-million; *DPH*, diphthamide.

The relationship between DPHs mRNA and clinicopathological features

Based on clinical data from TCGA, such as T stage (*Figure 3A*), N stage (*Figure 3B*), histological grade (G1, G2, G3, G4) (*Figure 3C*), pathological stage (stage I, II and stage III, IV) (*Figure 3D*), and OS (*Figure 3E*), the expression of *DPHs* were evaluated in HCC and normal liver tissue. Our research showed that HCC tissues exhibited significantly higher expression levels of *DPHs* compared to normal liver tissue. Analysis of the clinicopathological correlations between *DPHs* found interesting correlations. Specifically, *DPH2* exhibited correlations with T stage (P=0.005), race (P=0.03), gender (P=0.001), histological grade (P=0.008), and OS (P=0.01). *DPH3* demonstrated correlations with weight (P=0.004), histological grade (P=0.001), alpha-fetoprotein (AFP) levels (P<0.001), and OS (P=0.01) (*Table 3* and Table S1). Furthermore, *DPH5* displayed correlations with T stage (P=0.005), race (P=0.02), histological grade (P<0.001), and vascular invasion (P=0.02). *DPH6* showed correlations with histological grade (P<0.001), race (P=0.001), weight (P<0.001), and prothrombin time (P=0.006). Lastly, *DPH7* exhibited correlations with weight (P<0.001), age (P=0.02), height (P=0.008), BMI (P=0.03), histological grade (P<0.001), AFP (P<0.001) and vascular infiltration (P=0.02) (*Table 4* and Table S1).

Diagnostic and predictive value of DPHs in HCC

We evaluated the ability of *DPHs* as diagnostic indicators of HCC using ROC analysis. The results showed that *DPHs* had considerable diagnostic value for HCC, such as *DPH1* (AUC =0.623, 95% CI: 0.562–0.685; *Figure 4A*); *DPH2* (AUC =0.950, 95% CI: 0.923–0.977; *Figure 4B*); *DPH3* (AUC =0.893, 95% CI: 0.855–0.932; *Figure 4C*); and *DPH5* (AUC =0.924, 95% CI: 0.895–0.953, *Figure 4D*); *DPH6* (AUC =0.883, 95% CI: 0.846–0.919; *Figure 4E*); *DPH7* (AUC =0.962, 95% CI: 0.941–0.983; *Figure 4F*). We separated the HCC patient data from TCGA into high and low-expression groups based on median expression levels to further investigate the predictive significance of *DPHs* in HCC. Kaplan-Meier survival curves showed that patients had worse OS with high expression levels of *DPH2* (HR =1.84, 95% CI: 1.30–2.61, P<0.001; *Figure 4G*) and *DPH3* (HR =1.81, 95% CI: 1.27–2.57, P<0.001; *Figure 4H*). However, the OS of HCC patients was higher in those with high *DPH7* expression levels (HR =1.46, 95% CI: 1.03–2.07, P=0.03; *Figure 4I*), *DPH1*,*5*,*6* did not affect the prognosis of HCC patients (*Figure 4J-4L*).

To further explore the diagnostic value of *DPH2*,*3* in HCC, we performed univariate and multivariate Cox regression analyses using RNA-seq data and clinical information from the TCGA database.

We conducted univariate and multivariate Cox regression analyses using RNA-seq data and clinical information from the TCGA database to better understand the predictive importance of *DPHs* in HCC. The variables considered in our analysis were tumor node metastasis (TNM) stage, histological grade, gender, age, and *DPH* family gene expression levels. Our univariate Cox regression analysis showed a strong correlation between the expression of *DPH2* (HR =1.947, 95% CI: 1.371–2.766, P<0.001;

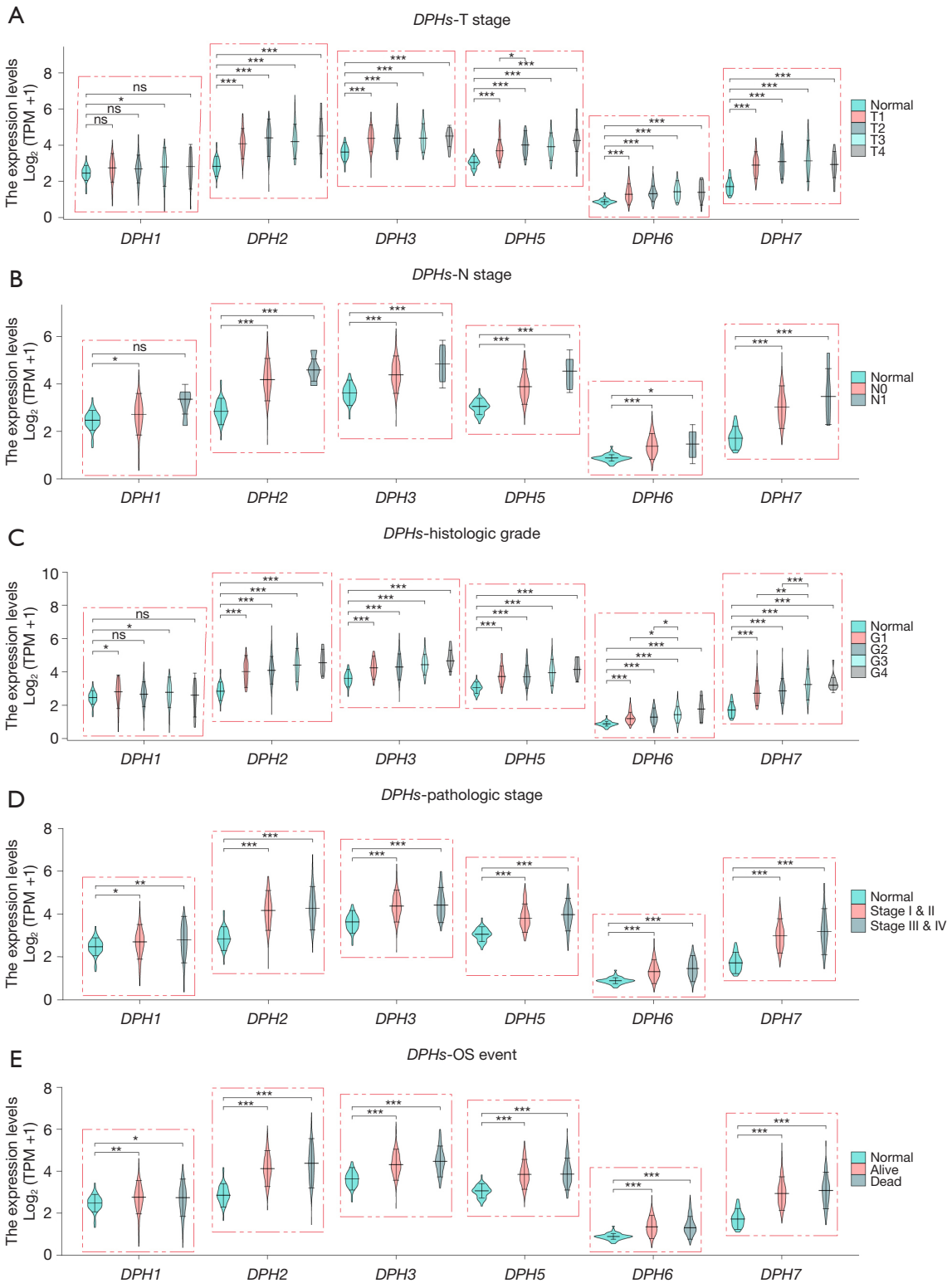

Figure 3 Correlation between *DPHs* expression and clinicopathologic features in HCC. Violin plots of *DPHs* expression were summarized according to (A) T staging, (B) N staging, (C) histologic grade, (D) pathologic stage, and (E) OS event. ns, P≥0.05; *, P<0.05; **, P<0.01; ***, P<0.001. *DPHs*, *DPH* genes; HCC, hepatocellular carcinoma; OS, overall survival; TPM, transcripts per-million; *DPH*, diphthamide.

Table 3 Clinicopathological characterization of *DPH1,2,3* in HCC patients from TCGA database

Characteristics	*DPH1* expression, n (%)			*DPH2* expression, n (%)			*DPH3* expression, n (%)		
	Low (N=185)	High (N=186)	P value	Low (N=185)	High (N=186)	P value	Low (N=185)	High (N=186)	P value
Pathologic T stage (N=368)			0.91			0.005			0.92
T1	90 (24.5)	91 (24.7)		103 (28)	78 (21.2)		90 (24.5)	91 (24.7)	
T2 & T3 & T4	94 (25.5)	93 (25.3)		79 (21.5)	108 (29.3)		92 (25)	95 (25.8)	
Histologic grade (N=366)			0.82			0.008			0.001
G1 & G2	115 (31.4)	117 (32)		127 (34.7)	105 (28.7)		131 (35.8)	101 (27.6)	
G3 & G4	68 (18.6)	66 (18)		54 (14.8)	80 (21.9)		52 (14.2)	82 (22.4)	
Race (N=359)			0.20			0.03			0.58
Asian	83 (23.1)	75 (20.9)		67 (18.7)	91 (25.3)		74 (20.6)	84 (23.4)	
Black or AA & White	92 (25.6)	109 (30.4)		109 (30.4)	92 (25.6)		100 (27.9)	101 (28.1)	
Weight (N=344)			0.73			0.08			0.004
≤70 kg	91 (26.5)	91 (26.5)		84 (24.4)	98 (28.5)		78 (22.7)	104 (30.2)	
>70 kg	78 (22.7)	84 (24.4)		90 (26.2)	72 (20.9)		95 (27.6)	67 (19.5)	
AFP (N=278)			0.62			0.50			<0.001
≤400 ng/mL	109 (39.2)	104 (37.4)		108 (38.8)	105 (37.8)		128 (46)	85 (30.6)	
>400 ng/mL	31 (11.2)	34 (12.2)		36 (12.9)	29 (10.4)		20 (7.2)	45 (16.2)	
OS event			0.26			0.01			0.01
Alive	115 (31)	126 (34)		132 (35.6)	109 (29.4)		132 (35.6)	109 (29.4)	
Dead	70 (18.9)	60 (16.2)		53 (14.3)	77 (20.8)		53 (14.3)	77 (20.8)	

HCC, hepatocellular carcinoma; TCGA, The Cancer Genome Atlas; AA, African American; AFP, alpha-fetoprotein; OS, overall survival; *DPH*, diphthamide.

Figure 5) and *DPH3* (HR =1.828, 95% CI: 1.287–2.597, P<0.001; *Figure 5*) with OS. Furthermore, our multivariate Cox regression analysis indicated that *DPH2* (HR =1.738, 95% CI: 1.093–2.763, P=0.02; *Figure 5*) and *DPH3* (HR = 1.833, 95% CI: 1.164–2.887, P=0.009; *Figure 5*) are independent predictors in HCC patients.

Methylation, mutation analysis, and GSEA of DPH2,3 in HCC

To understand the reasons for the higher expression of *DPH2,3* in HCC, we examined the mutations and methylation patterns associated with *DPH2,3* in HCC. Only a very small proportion of the 1,348 HCC samples in the cBioPortal database had genetic alterations, including 0.4% for *DPH2* and 0.3% for *DPH3*, and most of them were in the form of mutations and amplifications (*Figure 6A,6B*). Therefore, we propose that copy number amplification or mutation may not be the main cause of *DPH2,3* overexpression in HCC.

According to data from the TCGA database, levels of *DPH2,3* methylation in HCC were lower than those found in normal tissue (*Figure 6C,6D*). The MethSurv database revealed that the *DPH2* probes Body-Island-cg05050882 (HR =0.638, P=0.01; *Figure 6E*) and TSS1500-Island-cg20577479 (HR =0.556, P<0.001; *Figure 6F*) showed a poor prognosis in the hypomethylated group. Similarly, the *DPH3* probe 3'UTR-Open Sea-cg18650518 (HR =0.664, P=0.03; *Figure 6G*) demonstrated that the hypomethylation group had a poor prognosis. Based on these findings, we suggest that elevated *DPH2,3* expression in HCC patients may be linked to hypomethylation levels, which could adversely impact their prognosis.

To investigate the mechanism of *DPH2,3* in HCC, we performed a GSEA analysis. The results showed that *DPH2* was positively correlated with 12 pathways,

Table 4 Clinicopathological characterization of *DPH5,6,7* in HCC patients from TCGA database

Characteristics	*DPH5* expression, n (%)			*DPH6* expression, n (%)			*DPH7* expression, n (%)		
	Low (N=185)	High (N=186)	P value	Low (N=185)	High (N=186)	P value	Low (N=185)	High (N=186)	P value
Pathologic T stage (N=368)			0.005			0.07			0.07
T1	104 (28.3)	77 (20.9)		99 (26.9)	82 (22.3)		98 (26.6)	83 (22.6)	
T2 & T3 & T4	80 (21.7)	107 (29.1)		85 (23.1)	102 (27.7)		84 (22.8)	103 (28)	
Histologic grade (N=366)			<0.001			<0.001			<0.001
G1 & G2	134 (36.6)	98 (26.8)		136 (37.2)	96 (26.2)		136 (37.2)	96 (26.2)	
G3 & G4	49 (13.4)	85 (23.2)		48 (13.1)	86 (23.5)		45 (12.3)	89 (24.3)	
Race (N=359)			0.02			0.001			0.07
Asian	68 (18.9)	90 (25.1)		62 (17.3)	96 (26.7)		70 (19.5)	88 (24.5)	
Black or AA & White	112 (31.2)	89 (24.8)		113 (31.5)	88 (24.5)		108 (30.1)	93 (25.9)	
Weight (N=344)			0.23			<0.001			<0.001
≤70 kg	86 (25)	96 (27.9)		76 (22.1)	106 (30.8)		74 (21.5)	108 (31.4)	
>70 kg	87 (25.3)	75 (21.8)		97 (28.2)	65 (18.9)		98 (28.5)	64 (18.6)	
AFP (N=278)			0.67			0.054			<0.001
≤400 ng/mL	108 (38.8)	105 (37.8)		111 (39.9)	102 (36.7)		127 (45.7)	86 (30.9)	
>400 ng/mL	31 (11.2)	34 (12.2)		25 (9)	40 (14.4)		14 (5)	51 (18.3)	
OS event (N=371)			0.97			0.26			0.20
Alive	120 (32.3)	121 (32.6)		115 (31)	126 (34)		126 (34)	115 (31)	
Dead	65 (17.5)	65 (17.5)		70 (18.9)	60 (16.2)		59 (15.9)	71 (19.1)	

HCC, hepatocellular carcinoma; TCGA, The Cancer Genome Atlas; AA, African American; AFP, alpha-fetoprotein; OS, overall survival; *DPH*, diphthamide.

including cell cycle, DNA replication, homologous recombination, mismatch repair, pathogenic *Escherichia coli* infection, Fc gamma R mediated phagocytosis, P53 signaling pathway, gap junction, small cell lung cancer, pathways in cancer, neuroactive ligand receptor interaction and calcium signaling pathway (*Figure 7A,7B*), but with complement and coagulation cascades, peroxisome, peroxisome proliferators-activated recepto (PPAR) signaling pathway, drug metabolism cytochrome P450, oxidative phosphorylation and metabolism of xenobiotics by cytochrome P450 (*Figure 7C*) were negatively correlated. DPH3 was positively correlated with MAPK signaling pathway, focal adhesion, small cell lung cancer, cytokine cytokine receptor interaction, pathways in cancer, Wnt signaling pathway, ECM receptor interaction, pathogenic *Escherichia coli* infection, gap junction, primary immunodeficiency, Fc Gamma R mediated phagocytosis, and cell cycle (*Figure 7D,7E*). and negatively correlated with drug metabolism cytochrome P450, metabolism of xenobiotics by cytochrome P450, peroxisome, oxidative phosphorylation, drug metabolism other enzymes and PPAR signaling pathway (*Figure 7F*) were negatively correlated. The above results suggest that *DPH2,3* may be involved in the progression of HCC by influencing immune regulation, cell cycle, cancer pathways, and substance metabolism.

DPH2,3 is correlated to immune-related genes and immune cell infiltration

To investigate the immune action mechanism of *DPH2,3*, we analyzed its association with various types of immunity, including immunosuppressive, immunostimulatory, human leukocyte antigen (HLA), chemokine, and chemokine receptor genes. Our analysis showed a positive correlation between *DPH2,3* and most of the immune-related genes (*Figure 8A*). Additionally, we studied the correlation

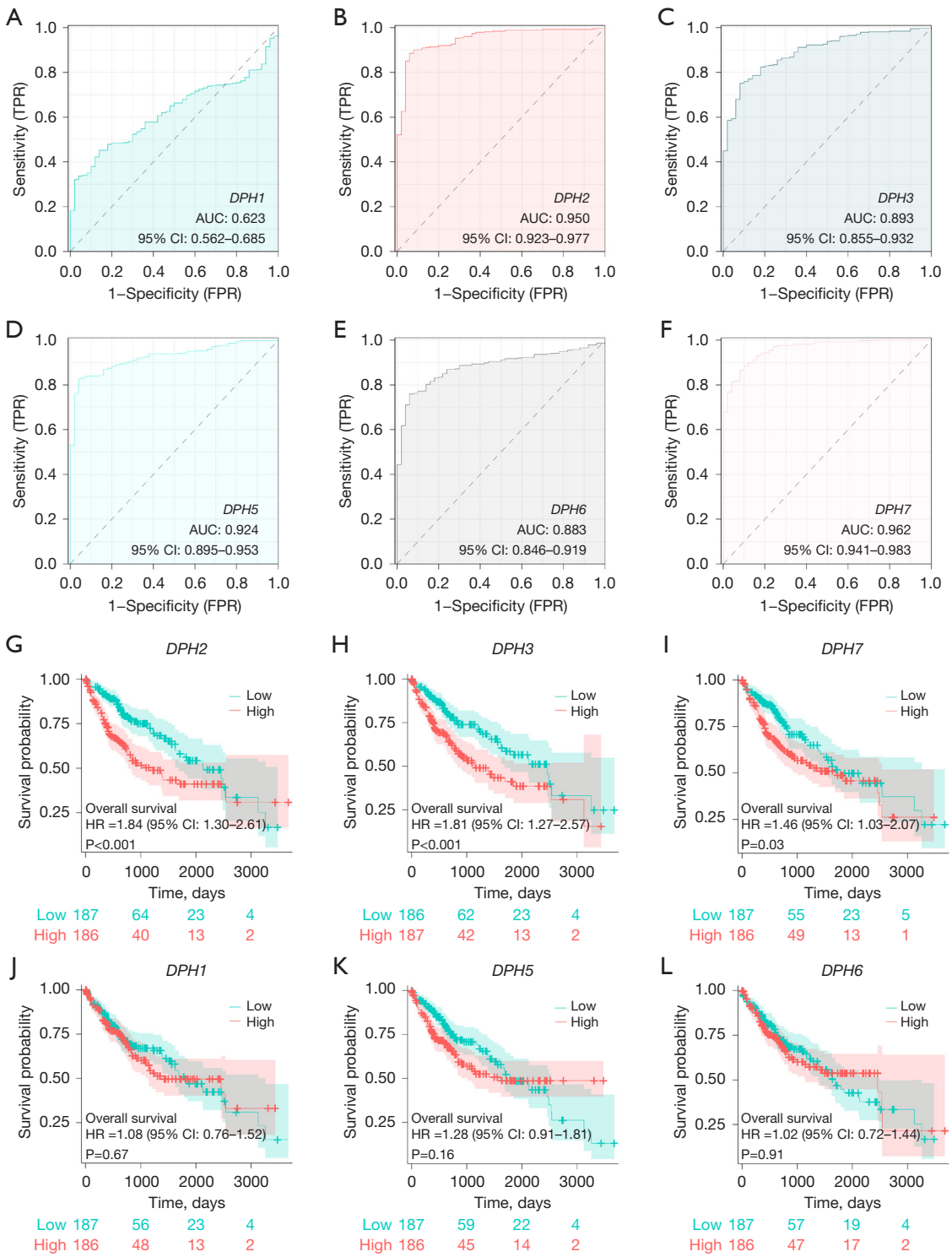

Figure 4 Diagnostic and prognostic value of *DPHs* in HCC. (A-F) ROC analysis indicates that *DPHs* expression has a good diagnostic value in HCC. (G-L) Kaplan-Meier curves showed the relationship between *DPHs* expression and OS, and the results indicated that the *DPH2*,*3*,7 high expression group had a worse prognosis. *DPHs*, *DPH* genes; HCC, hepatocellular carcinoma; ROC, receiver operating characteristic; OS, overall survival; TPR, true positive rate; FPR, false positive rate; AUC, area under curve; CI, confidence interval; HR, hazard ratio; *DPH*, diphthamide.

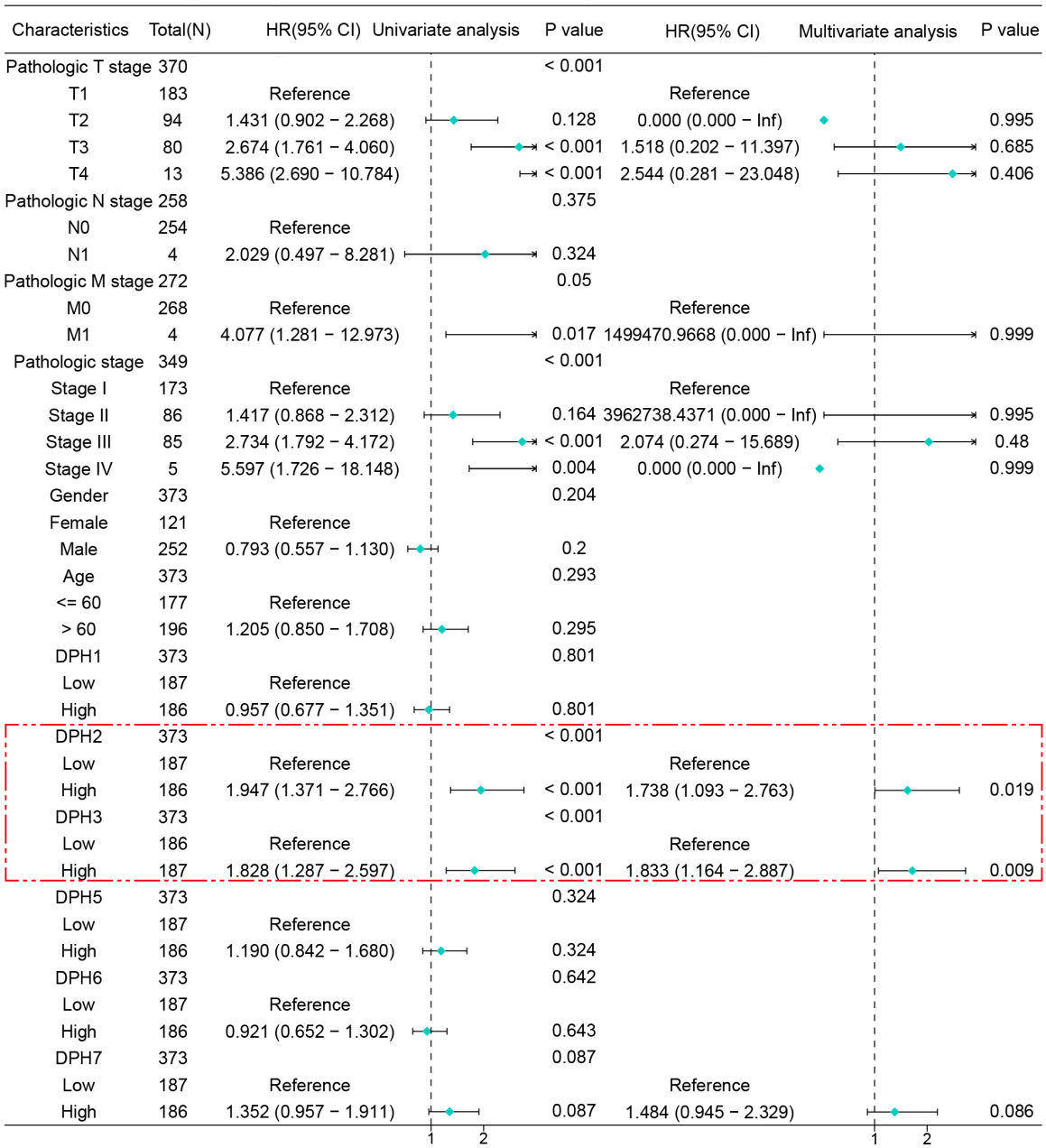

Figure 5 Univariate Cox regression analyses showed that *DPH2,3* was significantly associated with OS, and multivariate Cox regression analyses showed that *DPH2,3* was an independent prognostic factor. OS, overall survival; HR, hazard ratio; CI, confidence interval; *DPH*, diphthamide.

between *DPH2,3* and immune checkpoint molecules, such as *PDCD1* (*DPH2*: R=0.16, P=0.002; *DPH3*: R=0.204, P<0.001; *Figure 8B,8C*), *CD274* (*DPH2*: R=0.225, P<0.001; *DPH3*: R=0.126, P=0.02; *Figure 8D,8E*), *CTLA-4* (*DPH2*: R=0.201, P<0.001; *DPH3*: R=0.253, P<0.001; *Figure 8F,8G*), *LAG3* (*DPH2*: R=0.108, P=0.04; *DPH3*: R=0.118, P=0.02; *Figure 8H,8I*), *HAVCR* (*DPH2*: R=0.282, P<0.001; *DPH3*: R=0.276, P<0.001; *Figure 8J,8K*), and *TIGIT* (*DPH2*: R=0.155, P=0.003; *DPH3*: R=0.245, P<0.001; *Figure 8L,8M*), which are widely studied in HCC. Our analysis revealed a positive correlation between *DPH2,3* and these immune checkpoint molecules.

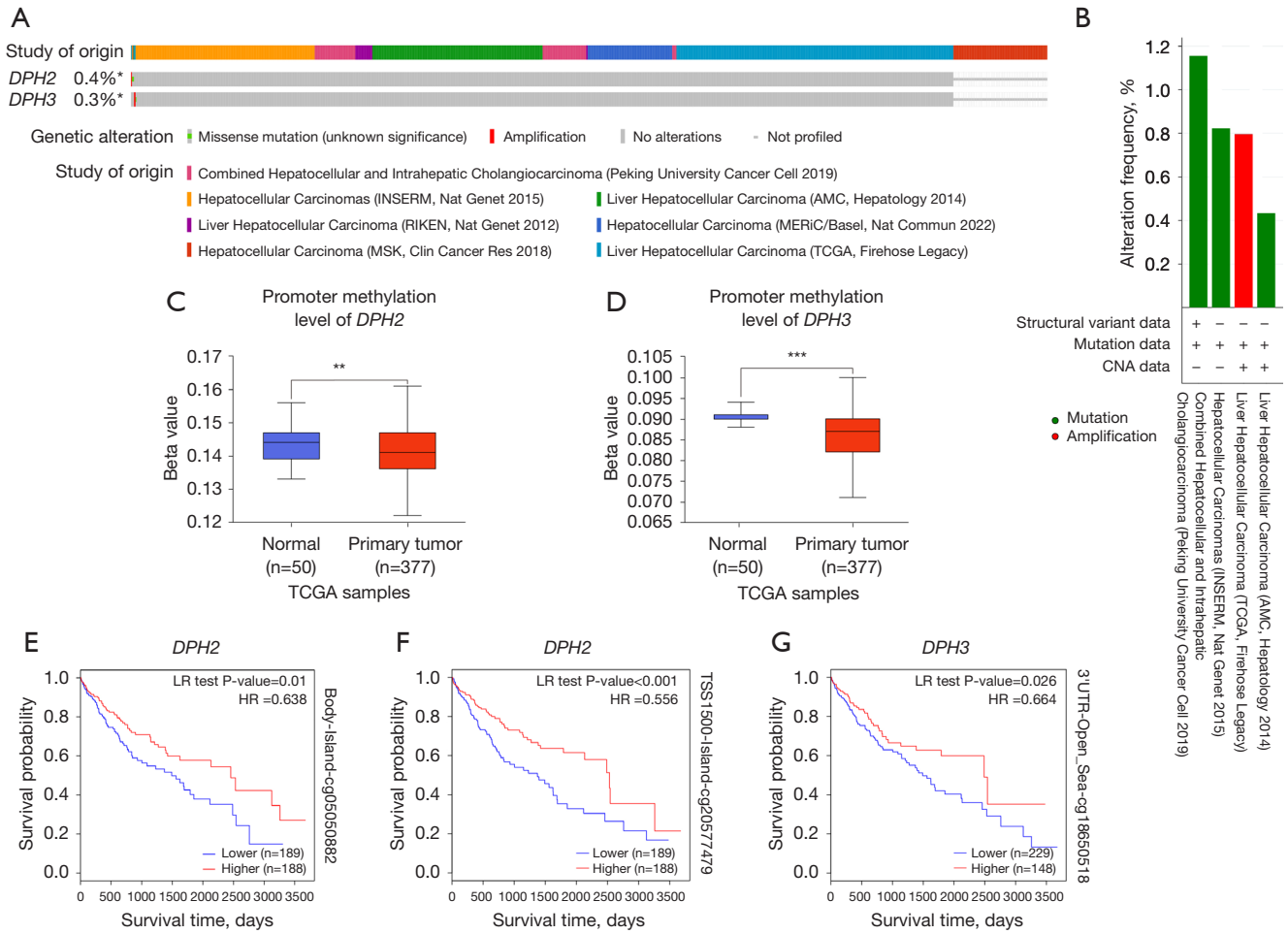

Figure 6 Analysis of *DPH2,3* gene mutation and methylation status suggests that *DPH2,3* high expression in HCC may be caused by its demethylation and affects its survival probability. (A,B) *DPH2,3* gene mutation data of HCC patients from the cBioPortal database (*, not all samples are profiled). (C) *DPH2* (**, P<0.01) and (D) *DPH3* (***, P<0.001) methylation data from the TCGA database. Kaplan-Meier survival analysis of (E) *DPH2* Body-Island-cg05050882, (F) *DPH2* TSS1500-Island-cg20577479, and (G) *DPH3* 3'UTR-Open_Sea-cg18650518 methylation sites from the MethSurv. HCC, hepatocellular carcinoma; TCGA, the cancer genome atlas; CNA, copy-number alterations; HR, hazard ratio; LR, likelihood ratio; *DPH*, diphthamide.

We investigated the correlation between *DPH2,3* expression and 24 different types of immune cells in HCC. Our findings revealed that *DPH2* was positively correlated only with Th2 cells (R=–0.345, P<0.001). On the other hand, it was negatively associated with Th17 cells (R=–0.309, P<0.001), CD8 T cells (R=–0.288, P<0.001), natural killer (NK) cells (R=–0.253, P<0.001), cytotoxic cells (R=–0.251, P<0.001), plasmacytoid dendritic cells (pDC) (R=–0.243, P<0.001), eosinophils (R=–0.233, P<0.001), dendritic cells (DC) (R=–0.232, P<0.001), mast cells (R=–0.197, P<0.001), neutrophils (R=–0.186, P<0.001), NK CD56dim cells (R=–0.176, P<0.001), and B cells (R=–0.171, P<0.001) (*Figure 9A*). On the other hand, *DPH3* was positively correlated with T helper cells (R=0.242, P<0.001), Th2 cells (R=0.202, P<0.001), macrophages (R=0.182, P<0.001), and activated dendritic cells (aDC) (R=0.104, P=0.02). However, it was negatively associated with Th17 cells (R=–0.339, P<0.001), NK cells (R=–0.163, P=0.002), and neutrophils (R=–0.116, P=0.02) (*Figure 9B*).

Next, we wanted to understand how *DPH2,3* expression affects immune cell infiltration in the TME. To this end, we divided HCC samples into two groups based on the expression level of *DPH2,3*-low-expression and high-expression groups. Further, we calculated the enrichment

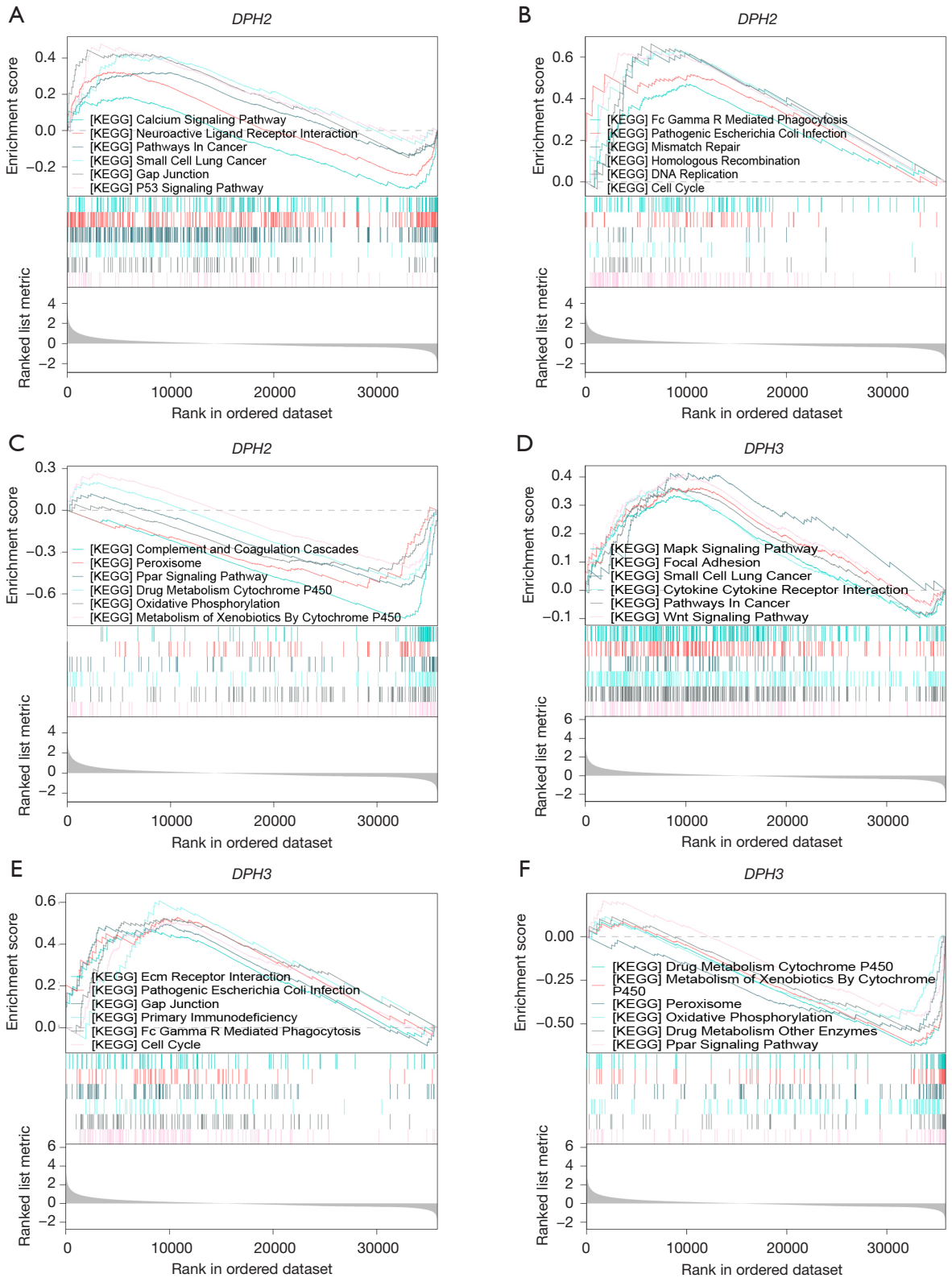

Figure 7 Enrichment plots from GSEA. Results of differential enrichment of gene in KEGG pathways with (A-C) *DPH2* and (D-F) *DPH3*. GSEA, gene sets enrichment analysis; KEGG, Kyoto Encyclopedia of Genes and Genomes; *DPH*, diphthamide.

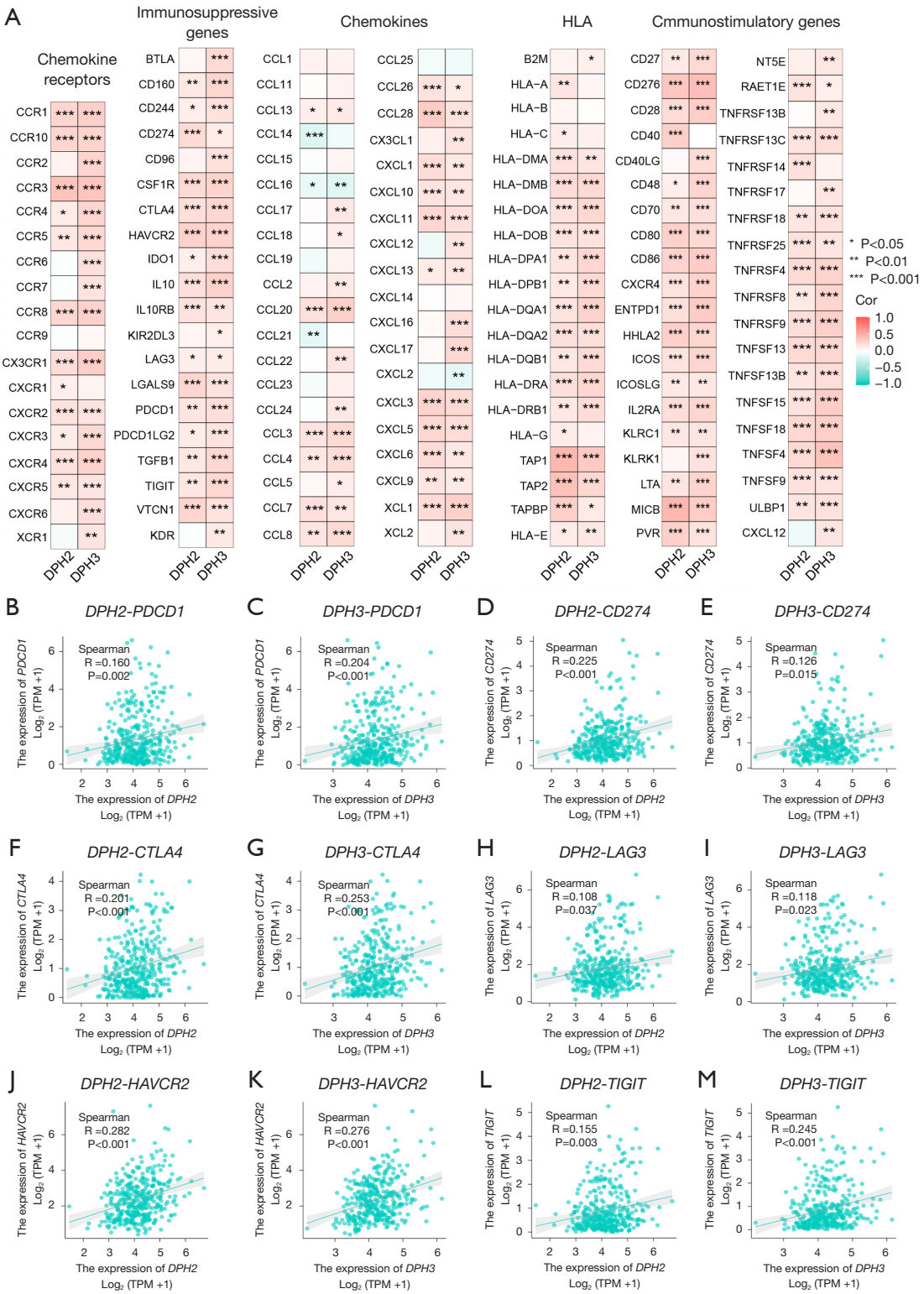

Figure 8 *DPH2,3* is significantly associated with immune-related genes. (A) Correlation of chemokine receptor genes, immunosuppressive genes, chemokine genes, human leukocyte antigen genes, and immunostimulatory genes with *DPH2,3*. *DPH2,3* was positively correlated with (B,C) PD-1 (*PDCD1*), (D,E) PD-L1 (*CD274*), (F,G) *CTLA-4*, (H,I) *LAG3*, (J,K) *HAVCR2* (TIM3) and (L,M) *TIGIT*. *, P<0.05; **, P<0.01; ***, P<0.001. HLA, human leukocyte antigen; *DPH*, diphthamide.

scores of immune cells in both groups. The results showed that the higher scores in the *DPH2* high-expression group were for Th2 cells, while the higher scores in the low-expression group were for 14 immune cell types including Th17 cells, CD8 T cells, and NK cells. These differences were statistically significant (all P<0.05; *Figure 9C*). Similarly, the higher scores in the DPH3 high-expression group were for T helper cells and Th2 cells, whereas the higher scores in the *DPH3* low-expression group were for 8 immune cell types including Th17 cells (all P<0.05; *Figure 9D*). Thus, our findings suggest that increased expression of *DPH2,3* in HCC affects the infiltration of immune cells in the TME, which may contribute to the survival of tumor cells.

Validation of DPHs mRNA expression in HCC cell lines and tissue samples using RT-qPCR

To verify the expression of *DPHs*, we first analyzed the mRNA levels in tissues using RT-qPCR. We found that the expression of *DPH1* (P<0.001; *Figure 10A*), *DPH2* (P<0.001; *Figure 10B*), *DPH3* (P<0.001; *Figure 10C*), *DPH5* (P<0.001; *Figure 10D*), and *DPH6* (P<0.001; *Figure 10E*), *DPH7* (P<0.001; *Figure 10F*) was elevated in HCC. Next, we analyzed the mRNA levels in tissues using RT-qPCR and found that *DPH1* expression was highest in MHCC97-H cells and relatively low in HCC-LM3 cells (*Figure 10G*), *DPH2* expression was highest in Hep-G2 cells and relatively low in Hep3B cells (*Figure 10H*), *DPH3* expression was highest in Hep3B cells and relatively low in SMMC-7721 cells (*Figure 10I*), *DPH5* had the highest expression in Hep-G2 cells and relatively low expression in HCC-LM3 cells (*Figure 10J*), *DPH6* had the highest expression in Hep-G2 cells and relatively low expression in SMMC-7721 cells (*Figure 10K*), and *DPH7* had the highest expression in Hep-G2 cells and relatively low expression in HCC-LM3 cells (*Figure 10L*). Overall, these results suggest that the *DPH* gene family is differentially expressed in HCC cells.

Discussion

Tumor cells promote their genesis and progression by reprogramming the translational process, in which high levels of protein synthesis play a key role in maintaining the metabolism of cancer cells (33). In this process, *eEF2* plays an important role (34). It has been found that Huanglian Jiedu Tang (HLJDD) may promote the phosphorylation of eEF2 by activating the AMPK, mTOR pathway, which inhibits the activity of eEF2 and thus prevents the progression of HCC (35). Notably, overexpression and enhanced activity of eEF2 in cancer are closely associated with cancer cell progression as well as early tumor recurrence (36,37). *DPHs* encode a key group of enzymes involved in the synthesis of diphthamide, a specifically modified histidine presents only in eEF2. the status of diphthamide influences the active state of eEF2 (11). Nevertheless, there is a lack of detailed studies reported on the expression pattern and the possible functions of *DPHs* in HCC.

A recent study of HCC based on a mouse model found that reduced *DPH1* expression was strongly associated with advanced disease and shorter survival time in patients with HCC. Nevertheless, *DPH1* deletion alone does not seem to be sufficient to trigger hepatocarcinogenesis. Strikingly, while the downregulation of *DPH1* limited translation prolongation rates, it increased total eEF2 levels (17). On the other hand, a study noted that the inactivation of either allele of *DPH1* or *DPH2* resulted in the accumulation of unmodified eEF2 and suggested that *DPH1* and *DPH2* were critical base for the synthesis of diphtheria (38). Meanwhile, DPH2,3 was found to maintain DPH1[4Fe-4S] cluster activity and reducibility, thus ensuring diphthamide function (39). In addition, a study revealed that the development and recurrence of basal cell carcinoma are associated with a *DPH3* promoter mutation, a mutation that also promotes migration and invasion of malignant cells (20). In our study, we observed up-regulation *DPH1* and *DPH2,3* expression, which may be a key mechanism adopted by tumor cells to maintain a high level of protein synthesis. DPH5 serves as a key enzyme required for the second step in the process of diphthamide synthesis. Even in cases where diphthamide synthesis is hindered or incomplete, the presence of DPH5 ensures the accuracy of eEF2 during translation (12). Another study revealed that diphthamide deficiency syndrome triggered by DPH5 deficiency is a novel autosomal recessive Mendelian disease (40). In our study, the expression of *DPH5* was significantly increased, which may be a key strategy adopted by tumor cells to ensure the accuracy of protein translation. In the third step of diphthamide synthesis, DPH6 and DPH7 are jointly involved in completing the process. Specifically, DPH7 is a methyl esterase that hydrolyzes the diphthyl ether generated by the methylation of DPH5, thus paving the way for the amidation of DPH6 to complete the final step of diphthamide synthesis (41). Strikingly, our study

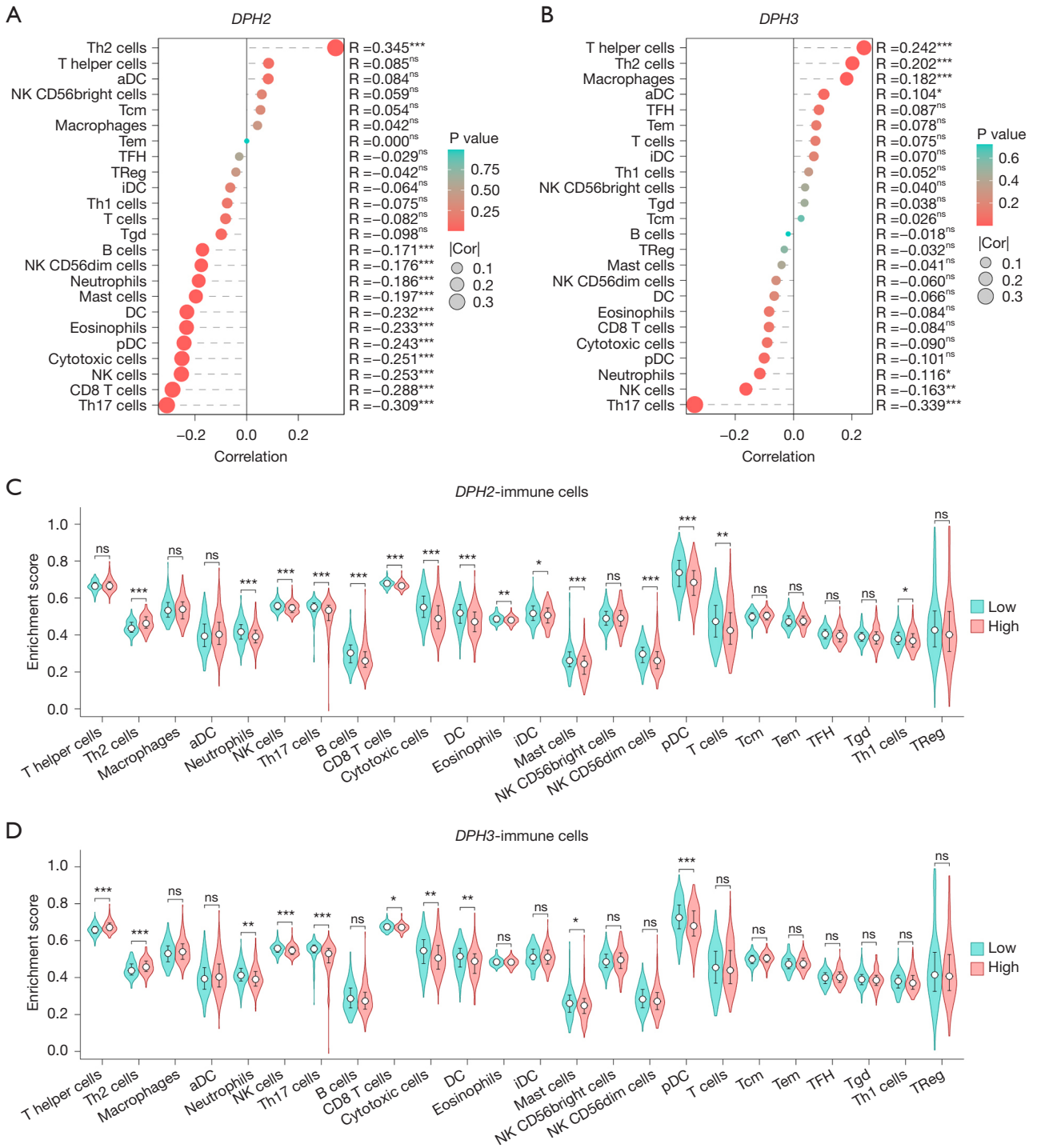

Figure 9 *DPH2,3* correlates with immune cell infiltration in HCC. Correlation between *DPH2* (A) and (B) *DPH3* expression and abundance of 24 tumor-infiltrating immune cell types. Enrichment scores of (C) *DPH2* and (D) *DPH3* high and low expression groups with 24 immune cell types. ns, P≥0.05; *, P<0.05; **, P<0.01; ***, P<0.001. HCC, hepatocellular carcinoma; NK, natural killer; pDC, plasmacytoid dendritic cell; aDC, activated dendritic cell; *DPH*, diphthamide.

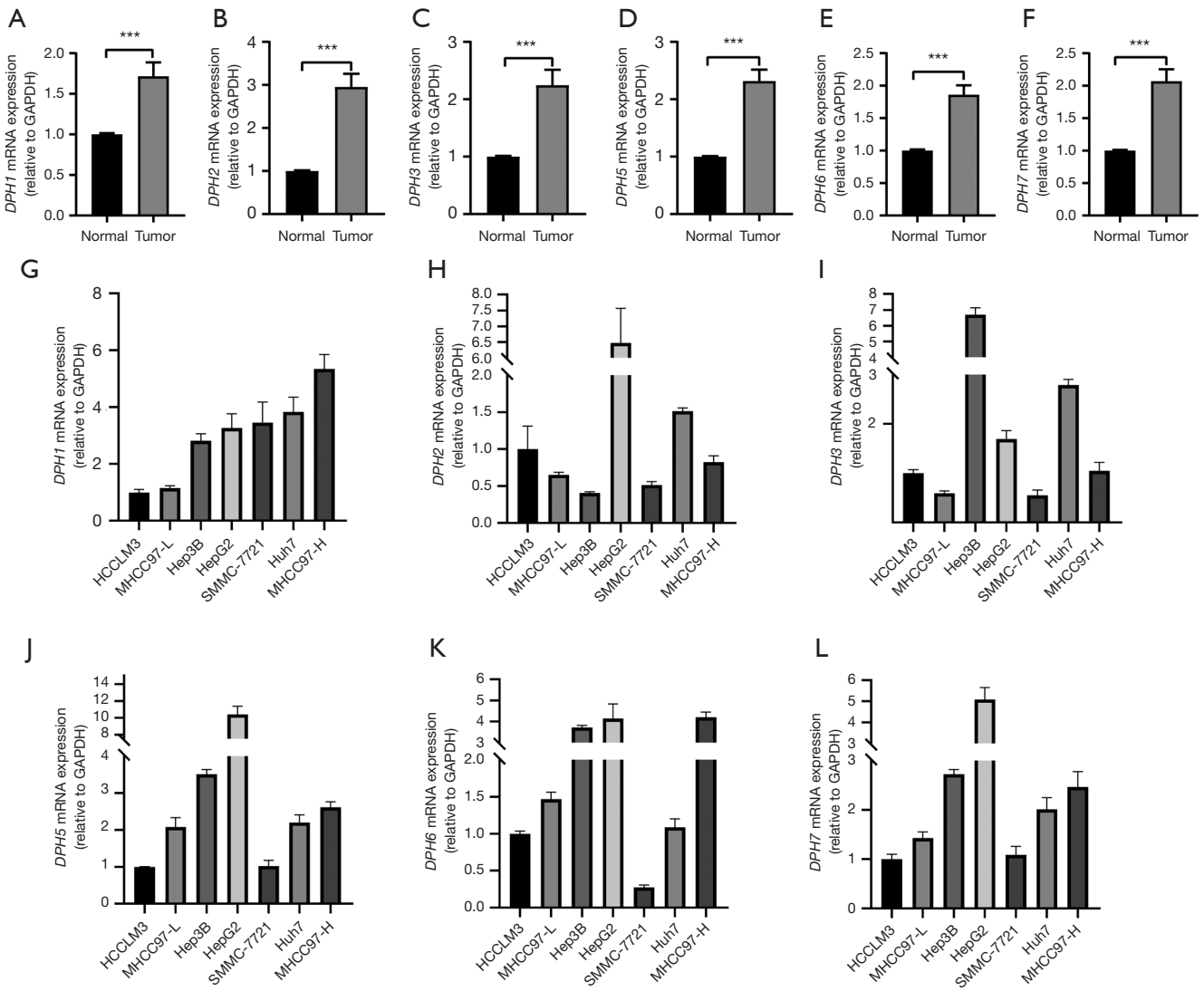

Figure 10 Expression of *DPHs* mRNA in HCC tissue samples and cell lines. (A-F) RT-qPCR analysis of *DPHs* mRNA expression in 18 HCC and normal liver tissue pairs. (G-L) RT-qPCR analysis of *DPHs* mRNA expression in 7 HCC cell lines. ***, P<0.001. DPHs, DPH genes; HCC, hepatocellular carcinoma; RT-qPCR, real-time quantitative polymerase chain reaction; *DPH*, diphthamide.

showed an increase in *DPH6* expression. However, the expression of *DPH7* was unstable, which may be caused by tissue variability. This needs to be verified with more experiments. Unexpectedly, the expression of *DPH7* was inconsistent with the expected results. This phenomenon may be related to its role as a potential negative regulator of RNA polymerase I (12). and it has been shown that the tumor's protein requirements for growth and cell division are dependent on RNA polymerase I (42). It was found that *DPH1*, *DPH2*, and *DPH5* play a crucial role in diphthamide synthesis. Although the deletion of diphthamide itself is not fatal, the deletion of *DPH3*, *DPH6*, and *DPH7* cannot be compensated by other genes (38,43). By analyzing the expression pattern of *DPHs* in pan-carcinomas, especially HCC, we found that the expression of *DPH1*,*7* was unstable, while the expression of *DPH2*,*3*,*5*,*6* increased. In this study, we used a sample of 18 cases to validate this expression pattern. We plan to expand the sample size in future studies to further validate and enhance our findings, ensuring their reliability and applicability on a larger scale. Based on this expression pattern, we hypothesized that HCC cells can ensure high levels of expression of their

proteins through this expression pattern, thus driving tumorigenesis and progression.

To gain insight into the mechanism of *DPHs* in HCC, we further investigated their association with clinicopathologic features. The results showed that *DPHs* were strongly correlated with histologic grade, especially *DPH2,3* was significantly correlated with OS. We also evaluated the efficacy of *DPHs* in the diagnosis and prognosis of HCC. The results of ROC analysis confirmed the high diagnostic value of *DPHs*. By Kaplan-Meier survival curve analysis, we found that patients with high expression of *DPH2*, *DPH3*, and *DPH*7 had a poor prognosis. Further univariate and multivariate Cox regression analyses also showed that the expression of *DPH2,3* was significantly associated with OS time. Thus, *DPH2,3* is not only valuable in the diagnosis of HCC but also independent factors affecting the prognosis of HCC patients. Next, we first used the cBioportal database to analyze the mutation status of these two genes, and then we performed an analysis of the promoter methylation status of *DPH2,3* genes and their prognosis with the help of the UALCAN database and MethSurv to explore the reasons for the increased expression of *DPH2,3* in HCC. The results suggested that in HCC, the overexpression of *DPH2,3* was likely to be caused by the hypomethylation status of their promoters rather than gene mutations. Furthermore, this hypomethylation status may be a key factor contributing to the poor prognosis of HCC patients. To gain more insight into the regulatory mechanisms of DPH2,3 in HCC, we performed a GSEA. The results showed that DPH2,3 were positively correlated with cell cycle, Fc Gamma R mediated phagocytosis, and pathways in cancer, whereas they were positively correlated with peroxisome, PPAR signaling pathway, drug metabolism cytochrome P450, oxidative phosphorylation and oxidative phosphorylation were negatively correlated. Therefore, we hypothesized that HCC cells may promote their growth and development by regulating the cell cycle, cancer-related pathways, and certain immune and metabolic pathways.

TME in HCC is highly immunosuppressive, comprising various cell types, cytokines, and other components that impair antitumor immunity (44). The *DPH* gene family, particularly *DPH2* and *DPH3*, may play a crucial role in regulating the immune microenvironment of HCC by influencing immune-related gene expression and immune cell distribution. To gain insight into the immune mechanisms of *DPH2,3* within HCC, we first investigated the relationship between mRNA expression of *DPH2,3* and the five major immune modalities, including chemokines receptor genes, immunosuppressive genes, chemokines genes, HLA genes, and immunostimulatory genes (43). in particular, we presented the association between *DPH2,3* and common immune checkpoints (PD-1, PD-L1, CTLA-4, LAG3, TIM3, and TIGIT) (45). A previous study has shown that therapeutic strategies for HCC targeting immune checkpoints are highly promising (46). Our results showed that *DPH2,3* was significantly and positively associated with most immune-related genes and common immune checkpoints. Despite the success of immune checkpoint inhibitors in treating HCC, drug resistance remains a significant issue, resulting in poor therapeutic outcomes (47). Our study indicates that high *DPH2/3* expression may inhibit anti-tumor cell activity by regulating immunosuppressive pathways (e.g., PD-1/PD-L1 and CTLA-4), enabling tumor cells to evade immune surveillance and attack. Therefore, silencing DPH2/3 expression may enhance the efficacy of immune checkpoint inhibitors against tumor cells. The presence of immune-associated cells in the TME has a major impact on the progression of HCC. Tumor cells employ a variety of strategies to evade immune detection and clearance (48). Effective antitumor immunotherapy relies on the synergistic action of the components of the immune system (49) and utilizes immune cells inside and outside the TME to localize and destroy cancer cells (50-52), where combinations of immune checkpoint inhibitors and immune cell therapy are effective (53). We hypothesize that HCC cells disturb the immune mechanism by overexpressing *DPH2/3*, enabling tumor cells to evade immune detection and clearance. By altering the distribution of immune cells within the immune microenvironment, tumor cells evade immune attack. Therefore, we conducted an in-depth study of the association of 24 immune-infiltrating cells with *DPH2,3* expression. The results showed that high *DPH2/3* expression was associated with an increase in various pro-tumorigenic immune cells, including Th2 cells, helper T cells, and macrophages. These cells promote tumor growth and metastasis by secreting pro-inflammatory and growth factors (e.g., IL-4, IL-10, and TGF-β). Conversely, high *DPH2/3* expression suppressed immune cells with anti-tumor effects, such as Th17 cells, CD8 T cells, and NK cells. These cells exert their effects by secreting cytotoxic factors (e.g., IFN-γ and TNF-α) and directly killing tumor cells (48,49). These results suggest that DPH2/3 modifies the immune status of the TME by adjusting the ratio and activity of immune cells, thereby influencing HCC progression. High *DPH2/3* expression predicts poor

prognosis for HCC patients. Targeting *DPH2/3* and its pathways may restore anti-tumor immune responses and enhance immunotherapy, thus improving patient survival. Therefore, *DPH2/3* is a potential immunotherapy target in HCC patients. Next, we will investigate the mechanisms of *DPHs* in tumors and conduct further experiments to verify their feasibility and effectiveness as therapeutic targets. These studies will aid in developing new therapeutic strategies and providing more effective treatment options for HCC patients.

Another concern is that when diphthamide is intact, the toxin causes ADP-ribosylation of the diphthamide, leading to blocked protein synthesis and thus cell death. Based on this, we hypothesized whether it would be possible to treat tumor cells by restoring their diphthamide integrity and then targeting the toxin to the tumor cells. Therefore, we will further investigate the mechanism of action of *DPHs* in tumors to explore their potential in the treatment of tumors.

Conclusions

Overall, HCC maintains its genesis and progression by finely regulating the expression patterns of *DPHs*. Particularly noteworthy, *DPH2,3* showed significant clinical value in the diagnosis and prognosis of HCC. Further studies revealed that *DPH2,3* plays crucial roles in the immune microenvironment and immunoregulation, which may make them potential therapeutic targets for immunotherapy.

Acknowledgments

We thank LetPub (www.letpub.com) for its linguistic assistance during the preparation of this manuscript.

Funding: This project was supported by the National Natural Science Foundation of China (No. 81903026), the Sichuan Science and Technology Program (No. 2024YFHZ0052), the National Health Care Commission (No. WA2021RW26), the Sichuan Medical Science and Technology Innovation Research Association (YCH-KY-YCZD2024-026), and the Science and Technology Development Program of the Affiliated Hospital of North Sichuan Medical College (No. 2022PTZK003).

Footnote

Reporting Checklist: The authors have completed the MDAR reporting checklist. Available at https://tcr.amegroups.com/article/view/10.21037/tcr-24-147/rc

Data Sharing Statement: Available at https://tcr.amegroups.com/article/view/10.21037/tcr-24-147/dss

Peer Review File: Available at https://tcr.amegroups.com/article/view/10.21037/tcr-24-147/prf

Conflicts of Interest: All authors have completed the ICMJE uniform disclosure form (available at: https://tcr.amegroups.com/article/view/10.21037/tcr-24-147/coif). The authors have no conflicts of interest to declare.

Ethical Statement: The authors are accountable for all aspects of the work in ensuring that questions related to the accuracy or integrity of any part of the work are appropriately investigated and resolved. The study was conducted in accordance with the Declaration of Helsinki (as revised in 2013). The study was approved by The Medical Ethics Committee of the Affiliated Hospital of North Sichuan Medical College (protocol No. 2023ER153-1). All patients who participated in the study provided written informed consent before the collection of tissue samples.

References

1. Ganesan P, Kulik LM. Hepatocellular Carcinoma: New Developments. Clin Liver Dis 2023;27:85-102.
2. Toh MR, Wong EYT, Wong SH, et al. Global Epidemiology and Genetics of Hepatocellular Carcinoma. Gastroenterology 2023;164:766-82.
3. Siegel RL, Giaquinto AN, Jemal A. Cancer statistics, 2024. CA Cancer J Clin 2024;74:12-49. Erratum in: CA Cancer J Clin 2024;74:203.
4. Vogel A, Meyer T, Sapisochin G, et al. Hepatocellular carcinoma. Lancet 2022;400:1345-62.
5. Kulik L, El-Serag HB. Epidemiology and Management

of Hepatocellular Carcinoma. Gastroenterology 2019;156:477-491.e1.
6. Sung H, Ferlay J, Siegel RL, et al. Global Cancer Statistics 2020: GLOBOCAN Estimates of Incidence and Mortality Worldwide for 36 Cancers in 185 Countries. CA Cancer J Clin 2021;71:209-49.
7. Llovet JM, Castet F, Heikenwalder M, et al. Immunotherapies for hepatocellular carcinoma. Nat Rev Clin Oncol 2022;19:151-72.
8. Llovet JM, De Baere T, Kulik L, et al. Locoregional therapies in the era of molecular and immune treatments for hepatocellular carcinoma. Nat Rev Gastroenterol Hepatol 2021;18:293-313.
9. Wang H, Shi F, Zheng S, et al. Feasibility of hepatocellular carcinoma treatment based on the tumor microenvironment. Front Oncol 2022;12:896662.
10. Zhang H, Quintana J, Ütkür K, et al. Translational fidelity and growth of Arabidopsis require stress-sensitive diphthamide biosynthesis. Nat Commun 2022;13:4009.
11. Mateus-Seidl R, Stahl S, Dengl S, et al. Interplay between reversible phosphorylation and irreversible ADP-ribosylation of eukaryotic translation elongation factor 2. Biol Chem 2019;400:501-12.
12. Uthman S, Bär C, Scheidt V, et al. The amidation step of diphthamide biosynthesis in yeast requires DPH6, a gene identified through mining the DPH1-DPH5 interaction network. PLoS Genet 2013;9:e1003334.
13. Liu S, Milne GT, Kuremsky JG, et al. Identification of the proteins required for biosynthesis of diphthamide, the target of bacterial ADP-ribosylating toxins on translation elongation factor 2. Mol Cell Biol 2004;24:9487-97.
14. Mayer K, Schröder A, Schnitger J, et al. Influence of DPH1 and DPH5 Protein Variants on the Synthesis of Diphthamide, the Target of ADPRibosylating Toxins. Toxins (Basel) 2017;9:78.
15. Erdogan MA, Ashour A, Yuca E, et al. Targeting eukaryotic elongation factor-2 kinase suppresses the growth and peritoneal metastasis of ovarian cancer. Cell Signal 2021;81:109938.
16. Zhu S, Liao M, Tan H, et al. Inhibiting Eukaryotic Elongation Factor 2 Kinase: An Update on Pharmacological Small-Molecule Compounds in Cancer. J Med Chem 2021;64:8870-83.
17. Tu WL, Chih YC, Shih YT, et al. Context-specific roles of diphthamide deficiency in hepatocellular carcinogenesis. J Pathol 2022;258:149-63.
18. Liu M, Yin K, Guo X, et al. Diphthamide Biosynthesis 1 is a Novel Oncogene in Colorectal Cancer Cells and is Regulated by MiR-218-5p. Cell Physiol Biochem 2017;44:505-14.
19. Maturo MG, Rachakonda S, Heidenreich B, et al. Coding and noncoding somatic mutations in candidate genes in basal cell carcinoma. Sci Rep 2020;10:8005.
20. Nawrocka PM, Galka-Marciniak P, Urbanek-Trzeciak MO, et al. Profile of Basal Cell Carcinoma Mutations and Copy Number Alterations - Focus on Gene-Associated Noncoding Variants. Front Oncol 2021;11:752579.
21. Yao T, Liu JJ, Zhao LJ, et al. Identification of new fusion genes and their clinical significance in endometrial cancer. Chin Med J (Engl) 2019;132:1314-21.
22. Vivian J, Rao AA, Nothaft FA, et al. Toil enables reproducible, open source, big biomedical data analyses. Nat Biotechnol 2017;35:314-6.
23. Uhlén M, Fagerberg L, Hallström BM, et al. Proteomics. Tissue-based map of the human proteome. Science 2015;347:1260419.
24. Chandrashekar DS, Karthikeyan SK, Korla PK, et al. UALCAN: An update to the integrated cancer data analysis platform. Neoplasia 2022;25:18-27.
25. Liu J, Lichtenberg T, Hoadley KA, et al. An Integrated TCGA Pan-Cancer Clinical Data Resource to Drive High-Quality Survival Outcome Analytics. Cell 2018;173:400-416.e11.
26. Cerami E, Gao J, Dogrusoz U, et al. The cBio cancer genomics portal: an open platform for exploring multidimensional cancer genomics data. Cancer Discov 2012;2:401-4.
27. Modhukur V, Iljasenko T, Metsalu T, et al. MethSurv: a web tool to perform multivariable survival analysis using DNA methylation data. Epigenomics 2018;10:277-88.
28. Subramanian A, Tamayo P, Mootha VK, et al. Gene set enrichment analysis: a knowledge-based approach for interpreting genome-wide expression profiles. Proc Natl Acad Sci U S A 2005;102:15545-50.
29. Love MI, Huber W, Anders S. Moderated estimation of fold change and dispersion for RNA-seq data with DESeq2. Genome Biol 2014;15:550.
30. Yu G, Wang LG, Han Y, et al. clusterProfiler: an R package for comparing biological themes among gene clusters. OMICS 2012;16:284-7.
31. Bindea G, Mlecnik B, Tosolini M, et al. Spatiotemporal dynamics of intratumoral immune cells reveal the immune landscape in human cancer. Immunity 2013;39:782-95.
32. Hänzelmann S, Castelo R, Guinney J. GSVA: gene set variation analysis for microarray and RNA-seq data. BMC Bioinformatics 2013;14:7.

33. Bilanges B, Stokoe D. Mechanisms of translational deregulation in human tumors and therapeutic intervention strategies. Oncogene 2007;26:5973-90.
34. Kovalski JR, Kuzuoglu-Ozturk D, Ruggero D. Protein synthesis control in cancer: selectivity and therapeutic targeting. EMBO J 2022;41:e109823.
35. Wang N, Feng Y, Tan HY, et al. Inhibition of eukaryotic elongation factor-2 confers to tumor suppression by a herbal formulation Huanglian-Jiedu decoction in human hepatocellular carcinoma. J Ethnopharmacol 2015;164:309-18.
36. Vasamsetti BMK, Liu Z, Park YS, et al. Muscarinic acetylcholine receptors regulate the dephosphorylation of eukaryotic translation elongation factor 2 in SNU-407 colon cancer cells. Biochem Biophys Res Commun 2019;516:424-9.
37. Zhang X, Hu L, Du M, et al. Eukaryotic Elongation Factor 2 (eEF2) is a Potential Biomarker of Prostate Cancer. Pathol Oncol Res 2018;24:885-90.
38. Stahl S, da Silva Mateus Seidl AR, Ducret A, et al. Loss of diphthamide pre-activates NF-κB and death receptor pathways and renders MCF7 cells hypersensitive to tumor necrosis factor. Proc Natl Acad Sci U S A 2015;112:10732-7.
39. Zhang Y, Su D, Dzikovski B, et al. Dph3 Enables Aerobic Diphthamide Biosynthesis by Donating One Iron Atom to Transform a [3Fe-4S] to a [4Fe-4S] Cluster in Dph1-Dph2. J Am Chem Soc 2021;143:9314-9.
40. Shankar SP, Grimsrud K, Lanoue L, et al. A novel DPH5-related diphthamide-deficiency syndrome causing embryonic lethality or profound neurodevelopmental disorder. Genet Med 2022;24:1567-82.
41. Lin Z, Su X, Chen W, et al. Dph7 catalyzes a previously unknown demethylation step in diphthamide biosynthesis. J Am Chem Soc 2014;136:6179-82.
42. Ferreira R, Schneekloth JS Jr, Panov KI, et al. Targeting the RNA Polymerase I Transcription for Cancer Therapy Comes of Age. Cells 2020;9:266.
43. Wu B, Fu L, Guo X, et al. Multi-omics profiling and digital image analysis reveal the potential prognostic and immunotherapeutic properties of CD93 in stomach adenocarcinoma. Front Immunol 2023;14:984816.
44. Shen KY, Zhu Y, Xie SZ, et al. Immunosuppressive tumor microenvironment and immunotherapy of hepatocellular carcinoma: current status and prospectives. J Hematol Oncol 2024;17:25.
45. Liu Z, Liu X, Liang J, et al. Immunotherapy for Hepatocellular Carcinoma: Current Status and Future Prospects. Front Immunol 2021;12:765101.
46. Oura K, Morishita A, Tani J, et al. Tumor Immune Microenvironment and Immunosuppressive Therapy in Hepatocellular Carcinoma: A Review. Int J Mol Sci 2021;22:5801.
47. Ladd AD, Duarte S, Sahin I, et al. Mechanisms of drug resistance in HCC. Hepatology 2024;79:926-40.
48. Hao X, Sun G, Zhang Y, et al. Targeting Immune Cells in the Tumor Microenvironment of HCC: New Opportunities and Challenges. Front Cell Dev Biol 2021;9:775462.
49. Paijens ST, Vledder A, de Bruyn M, et al. Tumor-infiltrating lymphocytes in the immunotherapy era. Cell Mol Immunol 2021;18:842-59.
50. Chakraborty E, Sarkar D. Emerging Therapies for Hepatocellular Carcinoma (HCC). Cancers (Basel) 2022;14:2798.
51. Ma S, Li X, Wang X, et al. Current Progress in CAR-T Cell Therapy for Solid Tumors. Int J Biol Sci 2019;15:2548-60.
52. Xie G, Dong H, Liang Y, et al. CAR-NK cells: A promising cellular immunotherapy for cancer. EBioMedicine 2020;59:102975.
53. Mizukoshi E, Kaneko S. Immune cell therapy for hepatocellular carcinoma. J Hematol Oncol 2019;12:52.

Cite this article as: Gao X, He K, Zeng Z, Yin Y, Huang J, Liu X, Xiang X, Li J. Integrative analysis of the role of the *DPH* gene family in hepatocellular carcinoma and expression validation. Transl Cancer Res 2024;13(8):4062-4084. doi: 10.21037/tcr-24-147

